RSC Chemical Biology

ROYAL SOCIETY OF CHEMISTRY

PAPER

View Article Online
View Journal | View Issue

Cite this: *RSC Chem. Biol.*, 2022, **3**, 1260

Extending the *in vivo* persistence of synthetic glycoconjugates using a serum-protein binder†

Gour Chand Daskhan, [a] Bruce Motyka, [bc] Roger Bascom, [bc] Hanh Thuc Tran, [a] Kesheng Tao, [bc] Lori J. West [bcd] and Christopher W. Cairo *[ac]

Synthetic glycoconjugates are used in the development of vaccines and the design of inhibitors for glycan–protein interactions. The *in vivo* persistence of synthetic glycoconjugates is an important factor in their efficacy, especially when prolonged interactions with specific cell types may be required. In this study, we applied a strategy for non-covalent association of an active compound with serum proteins for extension of glycoconjugate half-life in serum. The small molecule, AG10, has previously been used to extend the half-life of small molecules through its high affinity for transthyretin (TTR), a serum protein. Using a tetravalent polyethylene glycol (PEG)-based scaffold we developed a synthetic strategy for glycoconjugates that allowed for controlled addition of multiple tags, such as a TTR affinity tag or fluorophore. We designed a version of AG10 modified at the pyrazole core, named GD10, amenable to our conjugation strategy and introduced to glycoconjugates using a tri-functional linker. This approach allowed for attachment of GD10 and fluorophore tags, as well as carbohydrate antigens. We then tested the influence of the GD10 tag on glycoconjugate half-life *in vivo* using a mouse model. Our results suggest that the combination of the GD10 tag and the PEG scaffold extended the half-life of glycoconjugates by as much as 10-fold when compared to proteins of similar molecular weight. The GD10 tag was able to extend the half-life of similar glycoconjugates by as much as 2-fold. We observed a role for the terminal saccharide residue of the carbohydrate antigen and confirmed that conjugates were able to penetrate multiple compartments *in vivo* including bone marrow, lymph nodes, and other organs. The introduction of the GD10 tag did not obstruct the ability of conjugates to interact with lectin receptors. We conclude that serum protein binders can be used to extend the persistence of glycoconjugates *in vivo*.

Received 19th May 2022,
Accepted 22nd August 2022

DOI: 10.1039/d2cb00126h

rsc.li/rsc-chembio

Introduction

Glycans in biological systems are often found as components of high-molecular weight glycoproteins, proteoglycans, and polysaccharides; as a class, these molecules are referred to as glycoconjugates. Synthetic glycoconjugates are commonly used in targeting biomolecules which recognize the presentation of native glycans.[1–3] Synthetic glycoconjugates are used as vaccines and therapeutic proteins in a variety of applications.[4–7] High molecular weight glycoconjugates have some inherent advantages as biological therapeutics. First, glycoconjugates of sufficient size (1–50 kDa) have increased persistence due to reduced elimination through renal glomerular filtration.[8–10] Furthermore, the presence of certain terminal saccharide residues (*e.g.* galactose or sialic acid) can directly modulate the half-life of glycoconjugates by modifying their interaction with receptor-mediated clearance mechanisms (*e.g.* the asialoglycoprotein receptor, ASGPR).[8,11,12] Challenges associated with glycoconjugate therapeutics include synthesis of defined high-molecular weight targets and discrete copy numbers of glycans, attachment of pendant groups (*e.g.* fluorophores, toxins, adjuvants, or other labels), as well as purification and characterization.[13] Our group is interested in the design of glycoconjugates which can be used to target glycan-recognizing immune receptors *in vivo*.[14]

Previous reports have employed glycoconjugates containing CD22 ligands and B cell receptor (BCR)-specific small molecule

[a] *Department of Chemistry, University of Alberta, Edmonton, Alberta, T6G 2G2, Canada. E-mail: ccairo@ualberta.ca; Fax: +1 780 492 8231; Tel: +1 780 492 0377*
[b] *Department of Pediatrics, Alberta Transplant Institute, University of Alberta, Edmonton, Alberta, T6G 2E1, Canada*
[c] *Canadian Donation and Transplantation Research Program, University of Alberta, Edmonton, Alberta, T6G 2E1, Canada*
[d] *Departments of Surgery, Medical Microbiology & Immunology, and Laboratory Medicine & Pathology, University of Alberta, Edmonton, Alberta, T6G 2E1, Canada*

† Electronic supplementary information (ESI) available: Preparation of compound **8**, structure of **28**, and characterization data for intermediates and conjugates. See DOI: https://doi.org/10.1039/d2cb00126h

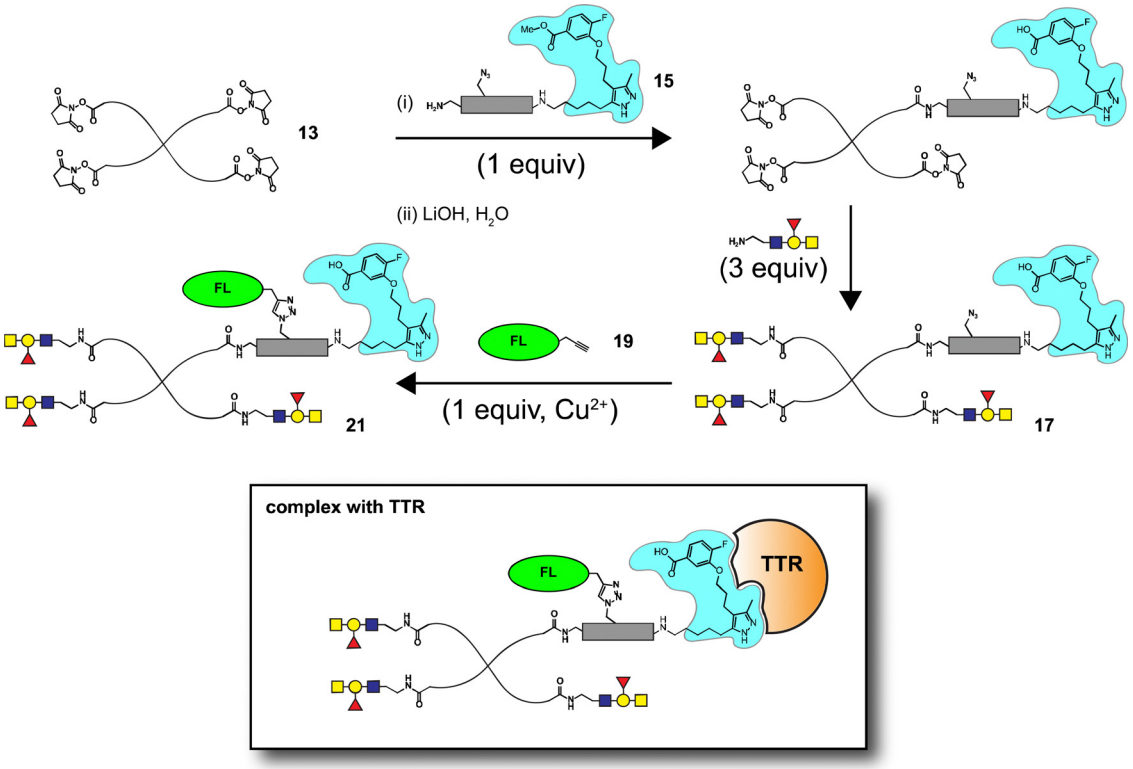

Scheme 1 Strategy for the synthesis of TTR-complexing glycoconjugates.

antigens as a strategy to suppress B cell activation.[15,16] We have extended this approach using human ABO blood group antigens to investigate the interaction of glycoconjugates with cells bearing a carbohydrate-binding BCR.[14] We selected a commercially available four-armed polyethylene glycol (PEG) scaffold that had been previously used for *in vivo* tolerance of protein antigens.[17] Part of our motivation for constructing ABO antigen-containing glycoconjugates was to explore their application as tolerogens – compounds that inactivate or suppress the B cell response to specific antigens.[18–20] Effective tolerogens must be able to penetrate into compartments where they can interact with immune cells, and must be persistent in serum.[17] Our previous strategy was able to generate glycoconjugates with the ability to bind and cluster BCRs and CD22 receptors *in vitro*, but we did not investigate their persistence *in vivo*.

To enable *in vivo* applications of these conjugates, we sought to establish new methods for significant extension of their half-life in serum. The PEG scaffold we selected has a molecular weight of 11.2 kDa (PDI, 1.025). Increased persistence of the compounds in serum is desirable as it is likely to enhance their function as tolerogens.[17] We considered an established strategy for extending the half-life of small molecules in serum which exploits small molecule binders of serum proteins.[21] This strategy non-covalently links the therapeutic molecule to serum proteins, which are found in high concentration and are cleared slowly. The most notable example of this approach used a small molecule transthyretin (TTR) binder, known as AG10, which has nanomolar affinity for the TTR complex.[21,22] The essential features for recognition of AG10 by TTR is a 3,5-dimethylpyrazole and a pendant benzoic acid group. The binding site for AG10 is located between two monomer units of the TTR tetramer.[23] Previous modifications of the AG10 binding epitope included changing the identity of the aromatic group or its substitution, as well as attachment of pendant groups from the pyrazole nitrogen or the aromatic side chain.[24] Symmetric modification of the 3,5-dimethylpyrazole ring to a 3,5-diethylpyrazole resulted in a major loss of activity.[24] Analogs that linked biorthogonal groups from the aromatic side chain have been pursued as TTR ligands for half-life extension (known as TLHEs).[21,22,25] The attachment of TLHEs to peptides resulted in large increases in circulating half-life by as much as 13-fold (from 3.5 to 46 min).[21] To the best of our knowledge, this approach has not been explored for the extension of glycoconjugate half-life in serum.

We hypothesized that an appropriate AG10 analog linked to a large glycoconjugate could significantly extend the persistence of these molecules in serum, a property likely to improve their activity as tolerogens. Herein, we report the development of a modification to our glycoconjugate synthesis that allows incorporation of two pendant groups (*e.g.* fluorophore and TTR-ligand) in addition to multiple copies of a carbohydrate antigen (*e.g.* ABO A-type II antigen) (Scheme 1). We describe an AG10 analog, referred to as GD10, containing a free amine linked through the C5 methyl group of the 3,5-dimethylpyrazole that maintained affinity for TTR. The GD10 analog, when attached to a synthetic glycoconjugate scaffold, was able to significantly extend persistence of the compound in serum in a murine

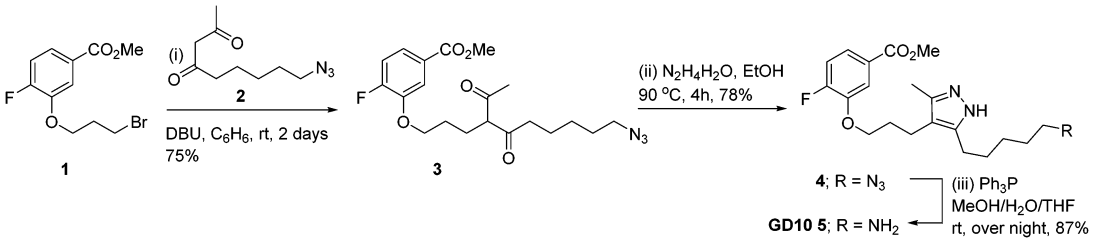

Scheme 2 Synthesis of amine-terminated analog 5 (GD10).

model. When combined with optimal glycan ligands on a PEG scaffold, our conjugates showed increases of as much as 2-fold of their persistence in mouse serum as compared to glyconjugates with similar functionalization. Furthermore, we investigated the fate of glycoconjugates using fluorescence imaging of whole animals; excised organs confirmed these materials were

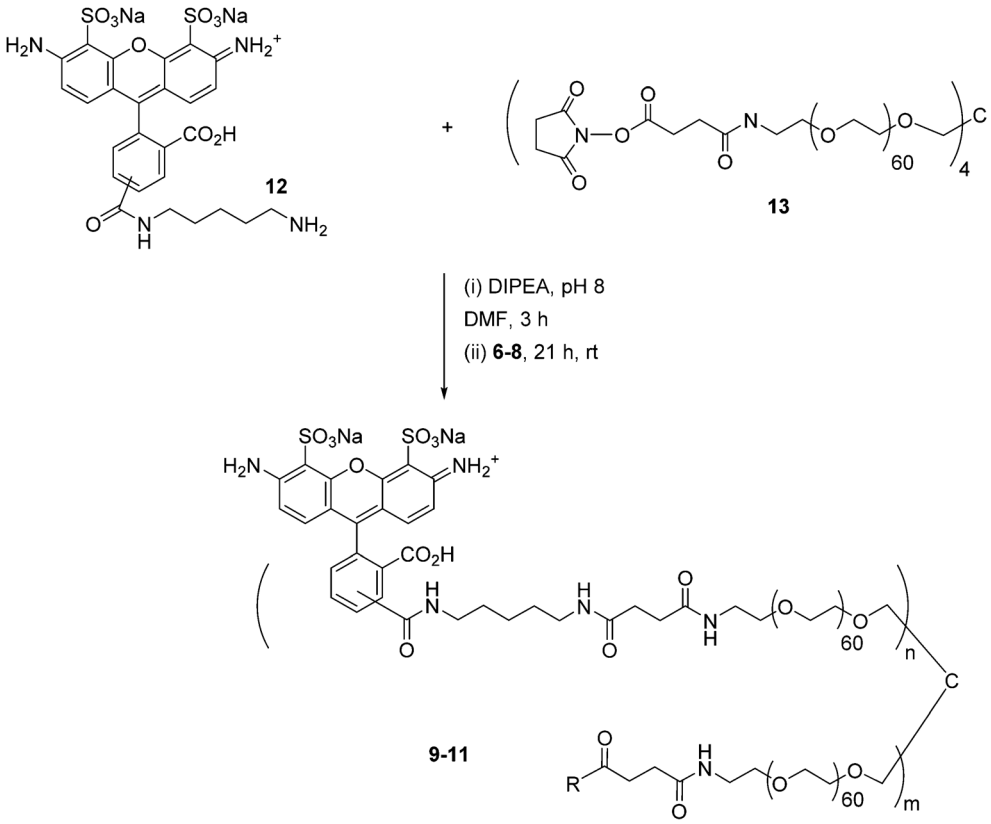

	Amine (R)	amination product	substitution ratio n:m	Yield (MW [kDa])
6*	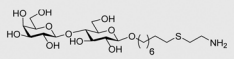	9*	1.3:2.7	90% (12.9)
7*	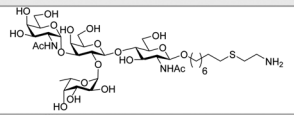	10*	0.6:3.4	90% (14.0)
8*	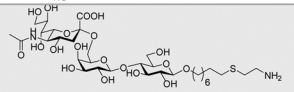	11	1:3	89% (13.8)

Scheme 3 Synthesis of AF-labeled glycoconjugate **11** using iterative amine coupling. * Previously reported.[14]

able to penetrate organs including lymph nodes and bone marrow.

Results and discussion

Synthesis of an amine-terminated AG10 analog, GD10

Co-crystal structures of AG10 analogs with WT-transthyretin (TTR or pre-albumin) have been reported.[22–24] Previous structure activity work found that the free acid, fluorine, and 3,5-dimethyl-1*H*-pyrazole groups are essential for binding.[24] While modification of both methyl groups of the pyrazole ring (3,5-diethyl-1*H*-pyrazole) showed poor activity, we reasoned that modification of a single position could maintain binding affinity. We planned a synthesis for an AG10 analog, GD10 **5**, containing a single modification of the pyrazole ring at C5 to introduce an amine while maintaining the fluorobenzoic acid moiety. The route began from compound **1** (Scheme 2), bearing a bromopropyl moiety, and was synthesized as previously reported.[22] Alkylation of compound **1** with DBU and azido derivative **2** in anhydrous benzene at room temperature afforded compound **3** in 75% yield. Treatment of a solution of compound **3** in ethanol with hydrazine hydrate under refluxing conditions for 4 h provided azido derivative **4** in a 78% yield after purification. Reduction of the azide moiety with triphenylphosphine in a mixture of methanol and water in THF at room temperature afforded amine-terminated GD10 **5** (Scheme 2) in good yield (50% overall).

Synthesis of amine-terminated carbohydrate antigens

Carbohydrate antigens suitable for attachment to a conjugate scaffold were prepared as free amines. For this study we

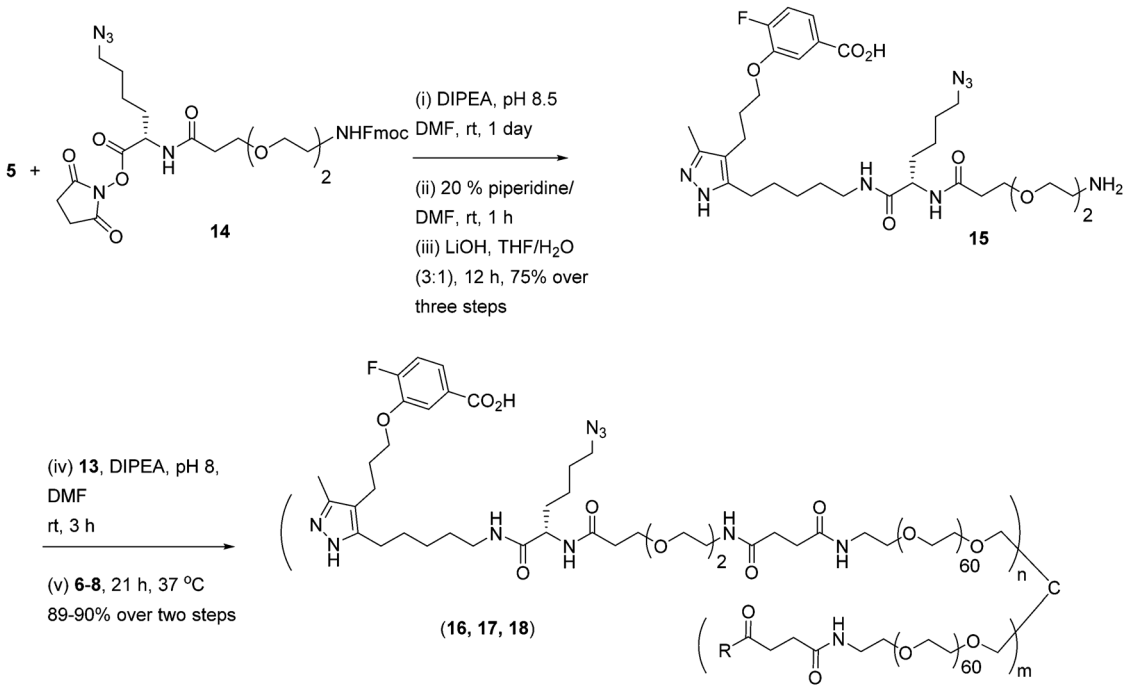

	Amine (R)	amination product	substitution ratio n:m	Yield (MW [kDa])
6*	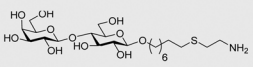	16	0.95:3.05	90% (13.0)
7*	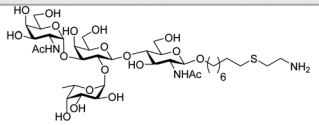	17	1.03:2.97	89% (14.1)
8*	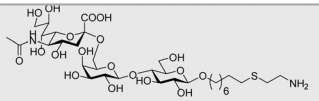	18	1:3	90% (13.8)

Scheme 4 Synthesis of tetravalent glycoconjugates (**16**, **17**, and **18**) with GD10 using iterative amine coupling.

generated lactose **6**, ABO A-type II **7**, and 6′-sialyllactose **8** (see ESI†). Amine-terminated carbohydrate antigens **6**, **7**, and **8** were synthesized first as alkene terminated glycosides, followed by a UV-promoted (λ = 254 nm) thiol–ene coupling (TEC)[26] with cysteamine as previously reported.[14]

Synthesis of AlexaFluor-labeled glycoconjugates

Synthesis of AlexaFluor 488-labeled (AF) lactose conjugate **9** (AF/lactose/PEG = 1.2 : 2.8 : 1, 13.0 kDa) and A-type II conjugate **10** (AF/A-type II/PEG = 0.6 : 3.4 : 1, 14.0 kDa) were reported previously.[14] A similar procedure was followed to prepare 6'-sialyllactose (6'-SL) conjugate **11** (AF/6'-SL/PEG = 1 : 3 : 1, 13.9 kDa). The conjugation strategy consisted of sequential amine coupling of AF-cadaverine **12** (λ_{ex} = 493 nm, λ_{em} = 516 nm) and carbohydrate antigen **8** with an NHS-activated PEG scaffold **13** (11.2 kDa) in the presence of DIPEA in DMF for one day at room temperature (Scheme 3). The ratio of substitution was determined using NMR and confirmed by mass spectrometry (see Experimental procedures).

Synthesis of tetravalent glycoconjugates containing GD10

Well-defined tetravalent glycoconjugates with GD10 were generated by developing a stoichiometrically-controlled conjugation strategy (Scheme 4). We note that this strategy results in a statistical mixture of different copy numbers on individual conjugates; however, we treated the final conjugates as an average based on NMR characterization (*vide infra*). Taking advantage of the compatibility of trifunctional linker **14** in bioconjugation, we decided to explore a sequential iterative amine coupling strategy for all three components to generate the target glycoconjugates. We previously used linker **14** for the synthesis of multivalent homo- and hetero-functional glycoconjugates presenting both BCR-specific ABO blood group antigens and sialosides as Siglec ligands that were able to co-cluster BCR and CD22 receptors *in vitro*.[14] We adapted our previous strategy by coupling of GD10 **5** with linker **14** to generate adduct **15** bearing an amine. This was followed by successive attachment of **15** and the carbohydrate amines (**6**, **7**, or **8**) onto the tetravalent NHS-activated PEG scaffold **13** under stoichiometric control. In the first step, GD10 **5** (1.25 equiv.) was coupled with NHS-activated linker **14** in the presence of DIPEA in anhydrous DMF at room temperature for one day. Subsequently, removal of the Fmoc-protecting group with 20% piperidine in DMF at room temperature followed by hydrolysis of the methyl ester was achieved with LiOH in a mixture of THF and water for 12 h. This one-pot, three-step reaction provided compound **15** in a 75% yield after purification by semipreparative RP-HPLC. The free amine **15** (1.0–1.25 equiv. per NHS-ester) was conjugated with NHS-activated PEG scaffold **13** (11.2 kDa) under similar

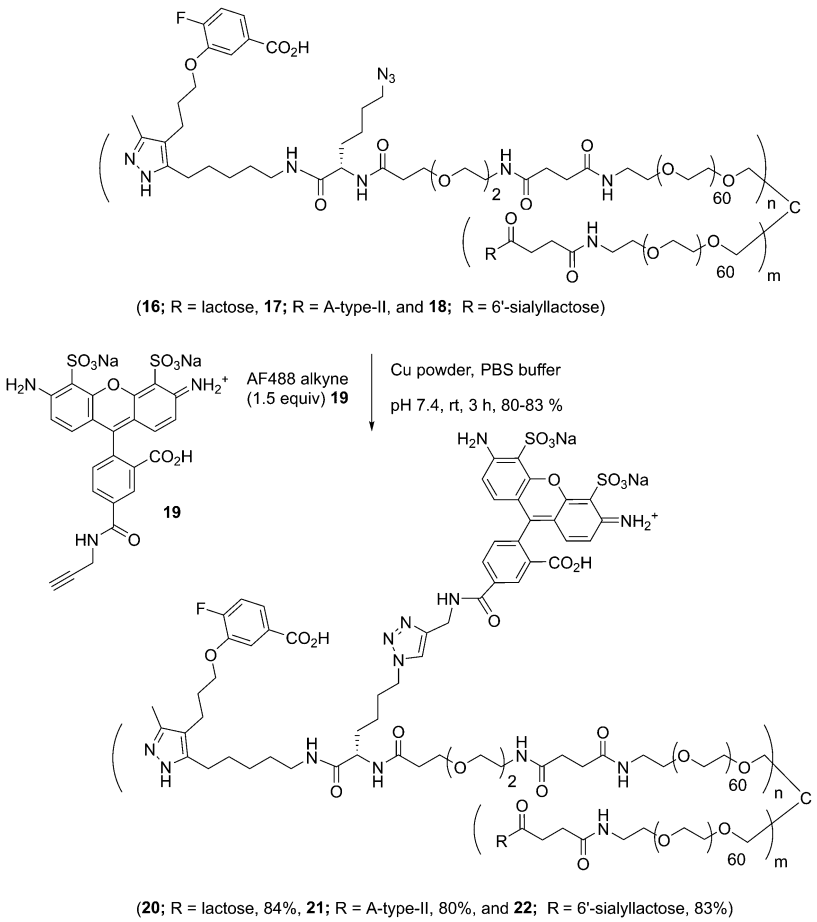

(**16**; R = lactose, **17**; R = A-type-II, and **18**; R = 6'-sialyllactose)

(**20**; R = lactose, 84%, **21**; R = A-type-II, 80%, and **22**; R = 6'-sialyllactose, 83%)

Scheme 5 Conjugation of AF to tetravalent scaffolds (**16**, **17**, and **18**) using CuAAC.

conditions to those above. After ~3 h, consumption of **15** was observed by TLC, subsequently the lactose amine **6** (3.5 equiv.) was immediately coupled with an intermediate NHS-PEG-GD10 adduct *via* amine coupling, and the reaction mixture was incubated at 37 °C for an additional 21 h.[14] After 24 h, the crude product was purified by C-18 chromatography to provide lactose-GD10 conjugate **16** (GD10/Lac/PEG = 0.95 : 3.05 : 1; 13.0 kDa) in 90% yield and purity over two-steps as a colorless powder after lyophilization. Substitution of GD10 and formation of the tetravalent structure with an azide moiety was confirmed by ^{1}H NMR and ^{19}F spectra. While the MALDI-TOF MS spectrum could suggest a loss of the azide group, the azide group was confirmed to be intact through subsequent CuAAC couplings (*vide infra*).[14]

The A-type II and 6'-sialyllactose amine-terminated compounds **7** and **8** were coupled with an intermediate NHS-PEG-GD10-adduct under similar coupling conditions described for conjugate **16** to provide A-type II-GD10 conjugate **17** (GD10/A-type II/PEG = 1.03 : 2.97 : 1, 14.1 kDa) and 6'-sialyllactose-GD10 conjugate **18** (GD10/6'-SL/PEG = 1 : 3 : 1; 13.8 kDa) in 89% and 90% respective yields after C-18 purification and lyophilization.[14] Analysis of the ^{1}H and ^{19}F NMR spectra, and MALDI-TOF mass spectra of **17** and **18** established the structure of the final targets (see Experimental procedures).

Synthesis of AF-labeled GD10-containing glycoconjugates

The glycoconjugates (**16–18**, 13.0–14.1 kDa) bearing GD10 and an azide moiety are primed for introducing additional tags for use in biological experiments using CuAAC ligation. To illustrate this, we prepared a new series of AF-labeled glycoconjugates with GD10 (**20–22**, 13.7–14.8 kDa). We adopted an established ligand-free Cu-power catalyzed CuAAC ligation method originally described by Danishefsky and co-workers,[27] with some modification (Scheme 5).[14] The CuAAC ligation of conjugate **16** was performed with commercially available AF alkyne **19** (1.5 equiv. per N_3) in the presence of Cu-powder (10 equiv. per N_3) in phosphate-buffered saline (PBS pH 7.4) under an N_2 atmosphere for ~3 h. The solid was removed by filtration and the crude product was purified by C-18 chromatography to afford conjugate **20** (13.7 kDa) in good yield. The appearance of triazole peaks at 8 ppm in ^{1}H NMR, and analysis of the MALDI-TOF mass spectrometry confirmed the structure of glycoconjugate **20**. A similar CuAAC ligation strategy was adopted for labeling of conjugates **17** and **18** with alkyne **19** under CuAAC ligation conditions to provide the desired AF-labeled glycoconjugates **21** (14.8 kDa) and **22** (13.7 kDa) in 80% and 83% respective yields after C-18 purification and lyophilization.

GD10 analogs bind to TTR with high affinity

We next sought to confirm that GD10 maintained affinity for its TTR protein target. The modification of the AG10 binding epitope in GD10 involved attachment through one of the methyl groups of the pyrazole ring. We investigated the binding of these analogs to TTR in PBS (pH 7.4) using a fluorescence polarization (FP) assay (Fig. 1). We first tested the direct binding of **24** to TTR by titrating a solution of the compound with increasing concentration of

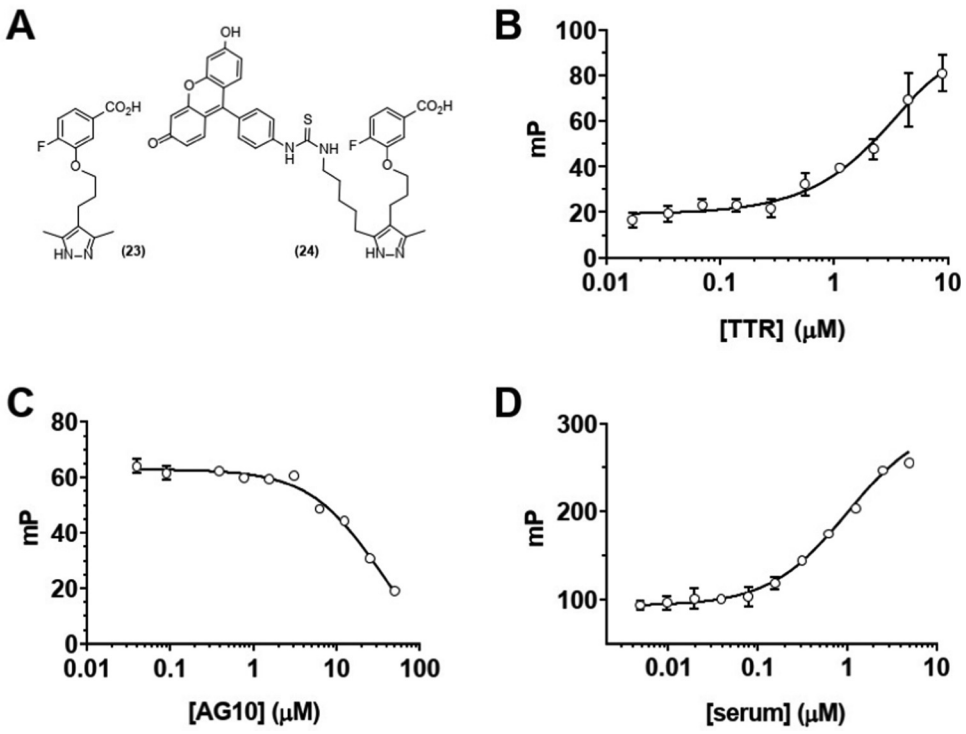

Fig. 1 Analogs of AG10 (**23**) and GD10 (**24**) bind to TTR and serum proteins. (A) Chemical structures of TTR ligands. (B) Direct binding of ligand **24** to TTR (0.017–9 μM) in buffer by FP (k_{app} = 5 μM); (C) competition of the **24**-TTR complex with increasing concentrations (0.04–50 μM) of AG10 analog **23** (k_{app} = 30 μM); (D) binding of compound **24** to mouse serum proteins (0.005–5 μM) (k_{app} = 1 μM).

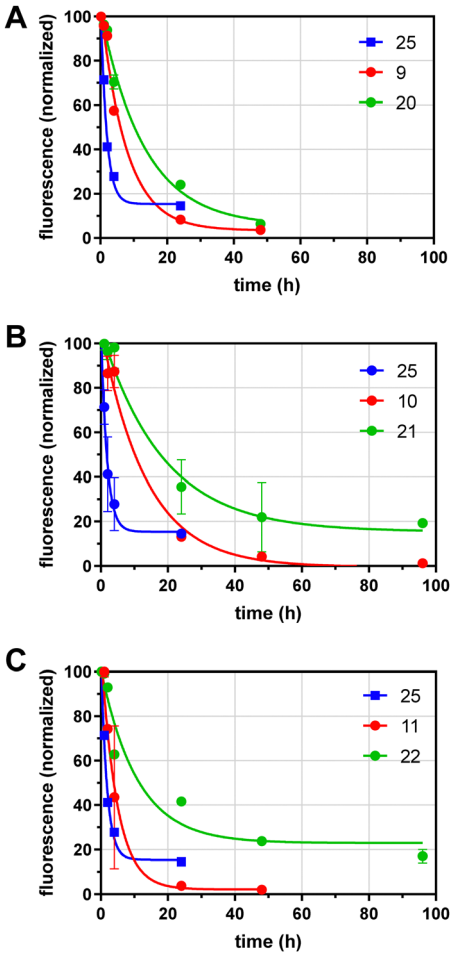

Fig. 2 *In vivo* half-life determinations for glycoconjugates. Compounds were injected i.v. into mice, and serum samples taken at indicated time points. The fluorescence of serum samples was compared to the initial reading (10 min) and fit to a single-phase exponential decay. Fluorophore labeled glycoconjugates are plotted in red, with the corresponding GD10 conjugate shown in green. Data for protein conjugate **25** (blue) are shown for comparison in all panels relative to (A) compound **9** and **20**; (B) compounds **10** and **21**; and (C) compounds **11** and **22**.

protein (Fig. 1B). These data confirmed that **24** bound directly to TTR (k_{app} = 5 μM). We note that this is lower than the reported affinity for AG10 (5 nM) and closer to that of diethylpyrazole analogs of AG10.[22] We next confirmed that complex formation between TTR and **24** could be disrupted by competition with the AG10 analog **23**. TTR was first pre-complexed to a GD10 analog with a fluorescent tag (**24**), followed by titration of unlabelled AG10 analog **23**. The loss of polarization observed was consistent with competitive binding of GD10 on TTR with a k_{app} = 30 μM (Fig. 1C). Finally, we considered that the hydrophobic structure of GD10 could interact with native serum proteins. We performed an analogous experiment by titrating mouse serum into a solution of **24** (Fig. 1D). We observed an increase in polarization consistent with direct binding of **24** to mouse serum proteins, similar to that of TTR alone (k_{app} = 1 μM). The observed lower k_{app} for **24** to serum over purified TTR may indicate that interactions with other serum proteins could affect clearance.

Glycoconjugates with GD10 have extended half-life in mouse serum

We next analyzed the effects of GD10 and glycoside incorporation on the clearance of glycoconjugates from mouse serum *in vivo*. To determine the half-life of conjugates in serum, fluorescent conjugates (100–400 μg) were injected into the saphenous vein in adult wild-type mice under isoflurane anesthesia and samples of serum were obtained over 96 h. The fluorescence remaining in serum was determined and normalized to the earliest timepoint (10 min) and the data fit to a single exponential decay (Fig. 2 and Table 1). We compared the clearance of our glycoconjugates to a protein of similar molecular weight (alpha-1-acidic glycoprotein, AGP) that was also labelled with AF **25** (dye : protein ratio of 1.2), which had a $t_{1/2}$ of 1.2 h. Conjugates containing lactose and an AF tag on the tetravalent PEG scaffold (**9**) had a longer $t_{1/2}$ of 5.3 h. A conjugate with 6′-SL and AF **11** had relatively rapid clearance with a $t_{1/2}$ of 3.3 h. Modification of the lactose conjugate with GD10 extended the $t_{1/2}$ to 9.1 h in the case of the lactose conjugate **20**, and we observed a similar effect for the AII conjugate **10** ($t_{1/2}$ of 9.3 h) which was extended to $t_{1/2}$ of 12.8 h after attachment of GD10 in conjugate **21**. Modification of the 6′-sialyllactose conjugate with GD10 in conjugate **22** extended the $t_{1/2}$ to 7.5 h. In all, we observed that 6′-sialylactose and lactose conjugates were cleared most rapidly, while AII conjugates were more persistent. The attachment of GD10 extended the $t_{1/2}$ in all cases, with increases of 2-fold or more. The most persistent conjugate in this series was **21**, which had more than 10-fold longer $t_{1/2}$ as compared to protein conjugate **25**. We note that the metabolic stability of the conjugates was not investigated in this study. Furthermore, we cannot rule out that a portion of the conjugates tested may have more than one copy of GD10 due to the statistical mixture that results from our strategy.

Table 1 The *in vivo* half-life in mouse serum of glycoconjugates with and without serum protein binders

Entry	Conjugate	Condensed name	Stoichiometry (n : m)	M_W (kDa)	*In vivo* half-life (h)
1	**9**[a]	AF/Lac/PEG	1.2 : 2.8	13.0	5.3
2	**20**	(GD10 + AF)/Lac/PEG	1 : 3	13.7	9.1
3	**10**[a]	AF/AII/PEG	0.6 : 3.4	14.0	9.3
4	**21**	(GD10 + AF)/AII/PEG	1 : 3	14.7	12.8
5	**11**	AF/6′SL/PEG	1 : 3	13.9	3.3
6	**22**	(GD10 + AF)/6′SL/PEG	1 : 3	14.5	7.5
7	**25**	AF-protein	1.2 (Dye : protein)	18.4	1.2

[a] Compounds previously reported.[14]

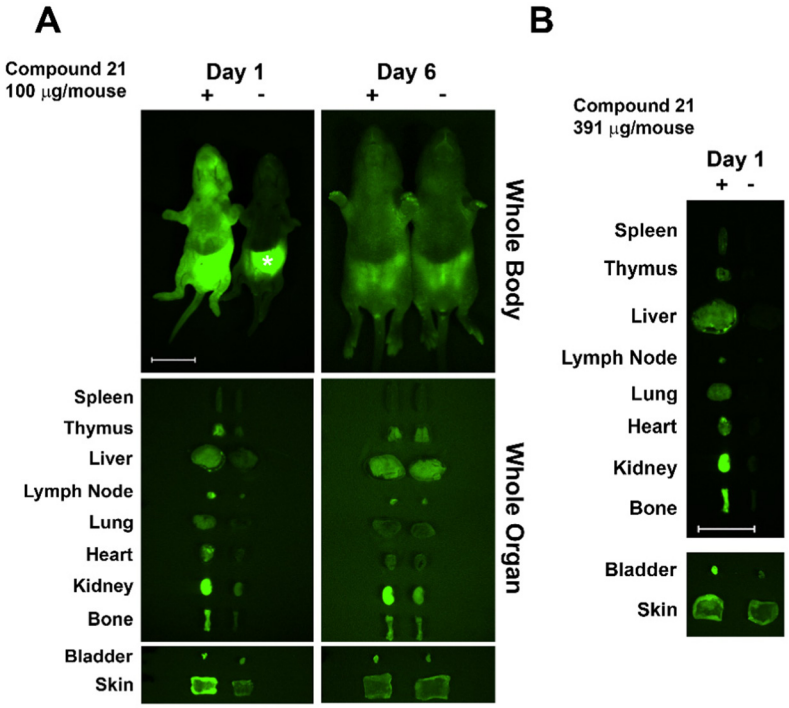

Fig. 3 Trafficking, fate, and clearance of injected A-type II antigen conjugates (**21**) in neonatal mice. Whole body and organ imaging of mice injected with fluorescent conjugate **21** or control animals was performed. Background autofluorescence was observed in controls due to stomach milk (*). Samples are labeled in the figure as (–) non-injected littermate control, and (+) animals injected with **21**. Scale bars: 10 mm (whole-body and organ imaging).

Distribution of fluorescent glycoconjugates in whole animals

Based on previous studies in C3H mice, we used newborn mice for clearance studies as newborns have decreased background autofluorescence in imaged tissues/whole animals *vs.* adults.[28] Glycoconjugate **21** was injected i.v. into newborn mice (within 24 h of birth) and its trafficking and clearance monitored. The glycoconjugate was injected at a concentration of 100 μg per mouse, similar to the dose used in previous studies.[29] Injected mice were euthanized at days one and six post-injection, and internal organs dissected and imaged next to those from non-injected littermate controls. The injected AF labeled-glycoconjugate was detected in host organs using an Olympus OV100 small animal imaging system. At day one post-injection **21** was detected in multiple organs with accumulation/sequestering in specific organs. Conjugate **21** sequestered mainly in kidney and bladder, followed by bone, with lower amounts detected throughout the mouse (Fig. 3). Sequestration in kidney and bladder indicate conjugate **21** was targeted for secretion. Skewed distribution in bone at day one may facilitate antigen exposure and tolerance induction, though additional higher resolution studies are needed. At day 6 post-injection almost all remaining AF signal was in kidney; however, a weaker signal was detected in other organs including bone. Injection of **21** at a higher dose (400 μg per mouse) resulted in higher fluorescence in bone at day one (Fig. 3B).

Glycoconjugates with GD10 maintain the ability to cluster BCR on ABL cells

In previous work, we had designed and tested glycoconjugates similar to those developed here featuring two carbohydrate epitopes that each engaged different receptors on B cells (BCR and CD22).[14] In that study, we found that four copies of a CD22 ligand were not sufficient to cluster the receptor, but that inclusion of four copies of a BCR ligand (the ABO A-type II antigen) resulted in co-clustering of both receptors. To investigate if the inclusion of a TTR ligand would interfere with clustering of a target receptor, we used **17** to synthesize a conjugate bearing GD10, the A-type II antigen, and 6'SL (**27**, Scheme 6). We then analyzed the cluster size of CD22 on B cells using confocal microscopy, and compared its activity to a previously reported conjugate **28** that was able to cluster CD22 (Fig. 4).[14] We observed that conjugate **28** was able to cluster CD22 on B cells as before. Treatment of the cells with conjugate **27**, or conjugate **27** in the presence of TTR, resulted in similar levels of CD22 clustering. The addition of TTR did not lead to a significant increase relative to treatment with **27** alone. These results confirm that the trivalent linker strategy developed here can provide conjugates that are able to engage cell surface receptors.

A-BCL cells were treated with 25 ng mL^{-1} PBS, **27**, **27** with TTR, or **28**,[11] then fixed and stained with *anti*-CD22 (mouse) and visualized using confocal microscopy. (**A**) Fluorescence images of representative cells are shown. (**B**) Cluster size on 20 individual cells was determined using particle analysis in ImageJ and plotted using the beanplot statistical package in R.[30] Each individual white horizontal line within the beanplot represents one single data point, the black horizontal line indicates the mean for each condition, and the dotted line indicates mean of all conditions within the plot. Populations

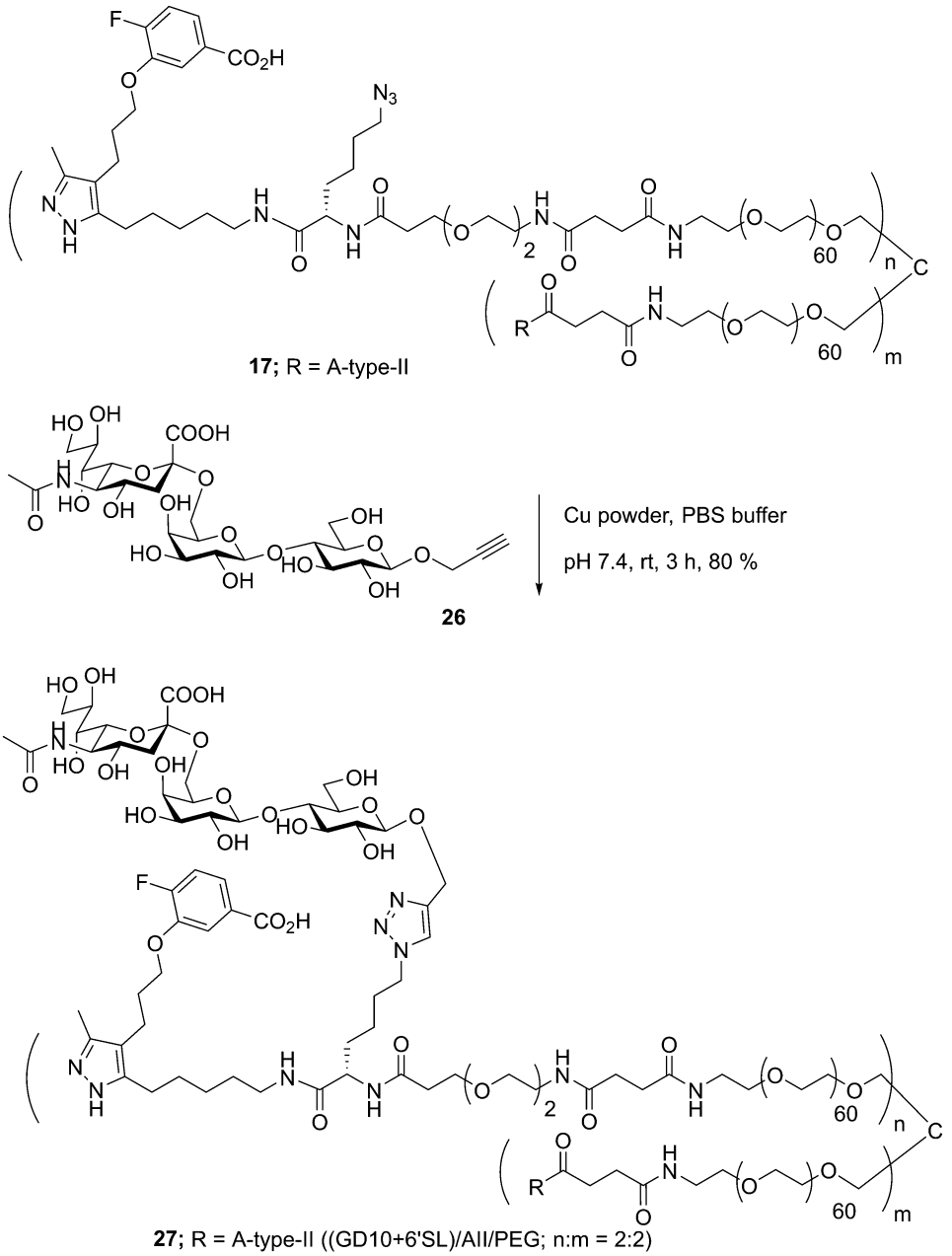

Scheme 6 Conjugation of 6′SL to tetravalent scaffold **17** using CuAAC ligation.

which were statistically different from control are indicated where $p < 0.0001$ with ****, as calculated using a student's *t*-test in GraphPad Prism.

Conclusions

In this study, we developed a TTR-binding small molecule, GD10, which is easily prepared as an amine in three steps (overall yield 50%). Our results indicate that asymmetric modification of the pyrazole ring of AG10 resulted in ligands with moderate affinity for TTR. This is the first demonstration of the extension of glycoconjugate half-life *in vivo* using this strategy. The inclusion of the GD10 tag was able to extend the serum half-life of conjugates by as much as 2-fold over the parent structure. PEG-based conjugates featuring human ABO blood group antigens and GD10 had half-lives that were extended by as much as 10-fold in serum relative to protein conjugates of similar molecular weight. Finally, we confirmed that these conjugates were able to penetrate multiple organs of animals including lymph nodes and bone and maintained the ability to engage cellular receptors. These results suggest this strategy may have enhanced capacity for induction of immune tolerance to carbohydrate structures.

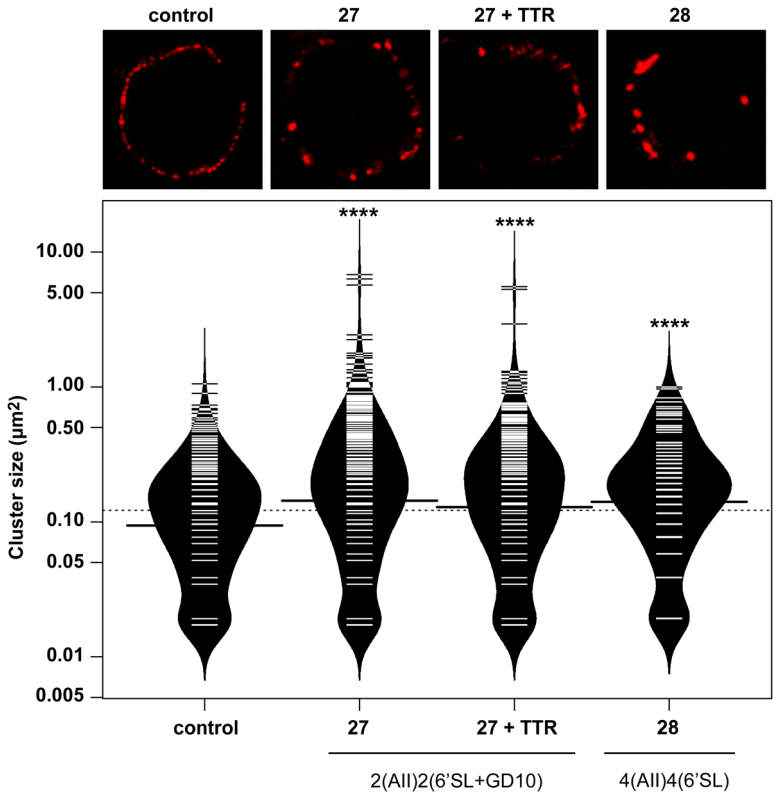

Fig. 4 Clustering of CD22 receptors by glycoconjugates and glycoproteins.

Experimental procedures

General methods

Reagents were purchased from commercial sources as noted and used without additional purification. Compounds **6**, **7**, **8**, and **26** as well as conjugates **9**, **10**, and **28** were previously reported (see ESI†)[14] Compound **23** was prepared as reported. NHS-activated PEG scaffold **13** was obtained from a commercial source (Laysan Bio Inc, Arab, Alabama). AF488 alkyne **19** was obtained from ThermoFischer Scientific. Cu-powder (<425 μm) and DIPEA were purchased from Sigma-Aldrich, Canada. Chloroform-d_1 and D_2O were purchased from Deutero GmbH. Other solvents (analytical and HPLC grade) and reagents were purchased from Aldrich and were used as received. Reactions were monitored by analytical TLC on silica gel 60-F254 (0.25 nm, Silicycle, QC, Canada). Developed TLC plates were visualized under UV lamp (λ_{max} = 254 nm) and charred by heating plates that were dipped in ninhydrin solution in ethanol, and acidified anisaldehyde solution in ethanol. Reaction products were purified by silica gel column chromatography (230–400 mesh, Silicycle, QC, Canada) or C-18 Sep-pak chromatography using ethyl acetate/hexane, or CH_2Cl_2/MeOH, and MeOH/H_2O as the elution solvents, respectively. Purifications were also performed by semi-preparative RP-HPLC with a Waters Delta 600 pump, and a Waters 600 controller with Empower 2 software. Eluted peaks were detected with a Waters 2420 evaporative light scattering (ELS) detector or a Waters 2996 photodiode array (PDA) detector (Waters Ltd, Mississauga, ON, Canada). Purifications were performed using solvent A: 0.01% TFA in water and solvent B: in CH_3CN at flow rate of 8.0 mL min^{-1} using a linear gradient of 2–50% solvent B in 20 min and UV detection at 214 nm. NMR experiments were conducted on a Varian 400, 500, or 600 MHz instruments in the Chemistry NMR Facility, University of Alberta. Chemical shifts are reported relative to the deuterated solvent peak or 3-(trimethylsilyl)-propionic-2,2,3,3-d_4 acid sodium salt as an internal standard and are in parts per million (ppm). Coupling constants (J) are reported in Hz and apparent multiplicities were described in standard abbreviations as singlet (s), doublet (d), doublet of doublets (dd), triplet (t), broad singlet (bs), or multiplet (m). The ratio of the incorporated GD10, carbohydrate structures and AF onto the PEG scaffold was determined by integration of the aromatic peaks of GD10 (7.63–7.07 ppm), anomeric peaks (5.30–4.40 ppm), PEG–COCH_2CH_2CO–(s, 2.49 or 2.50 ppm, 4H/per site), NHAc moiety of sialic acid (s, 1.98 or 1.99 or 2.00 ppm, 3H) and aromatic peaks of the fluorophore protons in ^{1}H NMR spectra. Electrospray mass spectra (ESI-MS) were recorded on Agilent Technologies 6220 TOF.

BALB/c and C3H mice (Charles River Laboratories, Sherbrooke, Québec, Canada) were housed in facilities at University of Alberta and cared for under guidelines of the Canadian Council of Animal Care. Animal protocols were approved by UofA Health Sciences Animal Care and Use Committee.

Synthesis of compound 2

To a suspension of NaH (270 mg, 60% mineral oil) in dry THF (12 mL) in a 50 mL flask, was added dropwise 2,4-diketopentane (0.58 mL, 5.8 μmol) at 0 °C under a nitrogen atmosphere.

The solution was stirred for 10 min and to this suspension was added dropwise *n*BuLi (2.2 mL, 2.5 M in hexane) and the resulting yellow solution was stirred for additional 15 min at 0 °C under an argon atmosphere. The reaction mixture was cooled to −30 °C and then was added 1-bromo-4-chlorobutane (0.67 mL, 5.8 μmol) slowly by syringe and the reaction mixture was stirred for additional ∼1 h at −25 °C. The reaction mixture was quenched with aqueous HCl (2N, 1 mL) and the solvents were removed under vacuum, diluted with diethyl ether (2 × 100 mL), washed with brine solution, dried over Na_2SO_4 and concentrated under vacuum to afford 9-chloro-4-oxo-2-nonanone as yellow oil which was used for the next reaction directly. NaN_3 (207 mg, 3.18 mmol) and NaI (10 mg) were added to a solution of 9-chloro-4-oxo-2-nonanone in dry DMF (5 mL) and the reaction mixture was heated to 60 °C overnight under an argon atmosphere. The solvent was removed, and the crude product was purified by silica gel chromatography using gradient elution (hexane to 1 : 9 v/v EtOAc/hexane) to afford compound **2** (867 mg, 76%) as a colorless oil. ^{1}H NMR (600 MHz, $CDCl_3$): δ 5.49 (s, 1H), 3.27 (t, J = 10.2 Hz, 2H), 2.89 (t, J = 10.8 Hz, 2H), 2.05 (s, 3H), 1.66–1.58 (m, 4H), 1.43–1.39 (m, 2H); ^{13}C NMR (125 MHz, $CDCl_3$): δ 193.82, 191.30, 99.83, 44.78, 38.04, 32.30, 26.46, 24.93, 24.87; (ESI): m/z $[M + H]^+$ calcd for C9H15N3O2 − H: 196.1092, found: 196.1091.

Synthesis of methyl-3-(3-(3-methyl-5-(5-azido pentanyl)-1*H*-pyrazol-4-fluorobenzoate 4

To a solution of compound **2** (299 mg, 1.51 mmol) and DBU (0.22 mL, 1.48 mmol) in dry benzene (2 mL) was added slowly a solution of **1** (220 mg, 0.75 mmol) in benzene (1 mL) under an argon atmosphere. The reaction mixture was stirred at room temperature for 2 days and filtered through Celite pad and solvent was concentrated under vacuum. The crude product was purified by silica gel chromatograph using gradient elution (hexane to 1 : 4 v/v EtOAc/hexane) to afford **3** as a colorless oil, which was directly used for the next reaction. To a solution of **3** in EtOH (2 mL) was added hydrazine monohydrate (73 μL, 2.27 mmol) and the reaction mixture was refluxed at 92 °C for 4 h. The reaction mixture was concentrated and purified by silica gel chromatograph using gradient elution (hexane to 1 : 4 v/v MeOH/$CHCl_3$) to afford desired compound **4** as a colorless oil. R_f = 0.38 (EtOAc/hexane = 2 : 3); ^{1}H NMR (400 MHz, $CDCl_3$): δ 7.40–7.38 (m, 1H), 7.28–7.25 (m, 1H), 7.11–7.07 (m, 1H), 3.99 (t, J = 6.0 Hz, 2H), 3.23–3.19 (m, 2H), 2.59–2.50 (m, 4H), 2.16 (S, 3H), 1.96–1.95 (m, 2H), 1.62–1.53 (m, 4H), 1.37–1.35 (m, 2H); ^{13}C NMR (125 MHz, $CDCl_3$): δ 167.67, 155.79, 153.79, 147.31, 147.23, 129.21, 129.18, 119.30, 119.24, 116.20, 116.05, 113.91, 113.76, 67.84, 51.34, 29.67, 28.78, 28.60, 26.56, 25.43, 18.89, 10.77; (ESI): m/z $[M + H]^+$ calcd for C20H26FN5O3 + H: 404.2092, found: 404.2204.

Synthesis of ethyl-3-(3-(3-methyl-5-(5-amino pentanyl)-1*H*-pyrazol-4-fluorobenzoate 5

To a solution of compound **4** (100 mg, 0.24 mmol) in a mixture of MeOH–H_2O–THF (3 mL, 1 : 0.5 : 1.5 v/v) was added PPh_3 (325 mg, 1.24 mmol) at room temperature and the reaction mixture was vigorously stirred for overnight. The solvents were removed and the crude product was purified by silica–gel chromatography using elution gradient ($CHCl_3$ to 2 : 3 v/v MeOH/$CHCl_3$) to afford compound **5** (81.4 mg, 87%) as a colorless oil. R_f = 0.28 (MeOH/$CHCl_3$ = 2 : 3); ^{1}H NMR (400 MHz, $CDCl_3$): δ 7.63–7.59 (m, 2H), 7.13–7.09 (m, 1H), 4.02 (t, J = 5.6 Hz, 2H), 3.89 (s, 3H), 2.90 (bs, 2H), 2.55–2.53 (m, 3H), 2.16 (s, 3H), 1.96 (bs, 6H), 1.63–1.62 (m, 4H), 1.38 (bs, 2H); ^{13}C NMR (125 MHz, $CDCl_3$): δ 166.17, 156.66, 154.64, 146.93, 146.85, 126.55, 126.52, 123.09, 123.03, 116.06, 115.91, 115.62, 115.59, 67.95, 52.26, 38.94, 29.82, 27.21, 26.82, 25.17, 24.56, 18.89, 10.45; (ESI): m/z $[M + H]^+$ calcd for C20H28FN3O3 + H: 378.2187, found: 378.2186.

Synthesis of conjugate 11

A mixture of AlexaFluor 488 cadaverine **12** (0.6 mg, 0.93 μmol, 1.05 equiv.) and NHS-activated PEG **13** (10 mg, 0.89 μmol, 1 equiv.) were dissolved in dry DMF (80 μL) and DIPEA and placed in a 0.5 mL centrifuge tube at room temperature. After ∼3 h, the 6′-sialyllactose amine **8** (2.37 mg, 2.90 μmol, 3.25 equiv.) was added and the reaction mixture was purged with argon and incubated at 23 °C for an additional ∼21 h. The solvent was removed and the crude product was purified by C-18 Sep-pak chromatography using gradient elution of H_2O to MeOH/H_2O (8 : 2 v/v) to provide conjugate **11** (11.0 mg, 89%) as a reddish-colored powder after lyophilization. Substitution of the PEG scaffold was determined by ^{1}H NMR integration of the underlined peaks to be Alexa Fluor : lactose : PEG = 1 : 3 : 1. ^{1}H NMR (500 MHz, D_2O): δ 8.28 (bs, 0.15H), 8.23 (bs, 0.6H), 8.19 (d, J = 7.2 Hz, 0.3H), 8.09–8.05 (m, 0.15H), 7.80 (s, 0.3H), 7.61 (s, 0.3H), 7.19 (d, J = 9.6 Hz, 0.6H), 7.01 (d, J = 9.0 Hz, 0.6H), 4.52 (d, J = 8.0 Hz, 1H), 4.48 (dd, J = 7.8 Hz, 1H), 4.41 (dd, J = 1.8, 12.0 Hz, 1H), 4.03–4.01 (m, 2H), 3.98–3.67 (bs, 273H), 3.60 (bs, 3H), 3.40–3.35 (m, 2H), 2.72 (t, J = 6.6 Hz, 2H), 2.64 (t, J = 6.6 Hz, 2H), 2.55–2.63 (m, 1H), 2.59 (bs, PEG–$COCH_2CH_2CO$–, 4H), 2.08 (s, 3H, NHAc), 1.82 (t, J = 12.0 Hz, 1H), 1.68–1.62 (m, 6H), 1.50–1.49 (m, 3H), 1.32–1.31 (m, 13H); ^{13}C NMR (125 MHz, D_2O): δ 175.85, 175.63, 175.57, 173.69, 164.73, 156.70, 156.66, 142.98, 120.80, 111.70, 111.52, 104.21, 102.89, 80.69, 75.69, 75.59, 74.60, 73.73, 73.59, 73.35, 72.52, 71.75, 71.63, 71.55, 70.56 (PEG CH_2–), 69.81, 69.46, 69.37, 69.09, 64.48, 63.72, 61.28, 52.75, 46.03, 40.81, 39.95, 39.70, 32.19 (2C), 32.04, 31.34, 29.71 (2C), 29.34, 29.16, 29.01, 28.85, 28.20, 25.97, 23.05; the MALDI-TOF spectrum showed the average mass centered at 13.8 kDa and expected average mass was 13.8 kDa.

Synthesis of compound 15

DIPEA (∼5.5 μL, 31.90 μmol) was added to a solution of GD10 amine **5** (10.0 mg, 26.51 mmol) and NHS-activated linker **14** (21.5 mg, 33.13 mmol) in anhydrous DMF (150 μL) at room temperature. The pH of the solution was adjusted to between 7.5–8.0 and the reaction mixture was incubated for one day at room temperature under anhydrous conditions. The solvent was removed, and the crude product was dried and treated with a 20% solution of piperidine–DMF (1 mL, 1 : 4) for 2 h. The solvent was removed under vacuum, and the crude product was

treated with LiOH (1.0 mg, 39.76 μmol) in H_2O/THF (2 mL, v/v = 3 : 1) for overnight at room temperature. The solvents were removed, and the crude product was purified by semipreparative RP-HPLC to afford compound **15** (13.8 mg, 75%) as colorless oil after lyophilization. Analytical RP-HPLC t_R = 12.7 min (gradient 5 to 100% B in 30 min). ^{1}H NMR (600 MHz, D_2O): δ 7.67 (q, J = 1.8 Hz, 1H), 7.65–7.62 (m, 1H), 7.23–7.19 (m, 1H), 4.26 (q, J = 6.0 Hz, 1H), 4.11 (t, J = 6.0 Hz, 2H), 3.75–3.73 (m, 2H), 3.68 (t, J = 6.0 Hz, 1H), 3.65–3.62 (m, 4H), 3.33 (s, 1H), 3.30 (bs, PEG–CH_2–, 8H), 3.17–3.09 (m, 2H), 2.75–2.71 (m, 3H), 2.53–2.50 (m, 2H), 2.36 (s, 3H), 2.05–2.02 (m, 2H), 1.74–1.66 (m, 1H), 1.65–1.59 (m, 2H), 1.58–1.51 (m, 2H), 1.49–1.40 (m, 2H), 1.37–1.33 (m, 2H); ^{13}C NMR (125 MHz, D_2O): δ 174.09 (2CO), 173.92, 163.14, 162.87, 147.49, 135.83, 123.36, 121.74, 119.41, 117.08, 114.82, 71.31, 71.24, 68.86, 68.60, 68.23, 54.69, 52.28, 40.33, 37.40, 32.87, 31.11, 30.77, 30.25, 30.10, 29.49, 27.71, 26.49, 24.17, 19.77, 12.57; ^{19}F–C NMR (400 MHz, D_2O): δ −75.50; (ESI): m/z $[M + H]^+$ calcd for C33H51FN8O7 + H: 691.3938, found: 691.3933.

General procedure for conjugation of compound 15 and amine-terminated carbohydrate with PEG scaffold 13

A mixture of compound **15** (1.0–1.25 equiv.) and NHS-activated PEG scaffold (**13**, 10 mg, 1 equiv.) were dissolved in anhydrous DMF (~80–90 μL) and placed in a 0.5 mL centrifuge tube at room temperature. DIPEA (1–1.25 equiv.) was added to adjust pH of the solution ~7.5–8.0 and the reaction mixture was incubated at room temperature. Consumption of compound **15** and progress of conjugation was monitored by TLC and LC-MS/MS analysis. After ~3 h, the carbohydrate amine (3.0–3.5 equiv.) was added and the solution was incubated at 23 °C for additional ~21 h. The solvent was removed under vacuum, and the crude product was purified by C-18 Sep-pak chromatography using H_2O to H_2O/MeOH (~3 : 7, v/v) as an eluent to afford azido-terminated GD10 conjugate as a colorless powder after lyophilization.

General procedure for CuAAC ligation

A solution of an azido-terminated GD10-PEG-conjugate (1 equiv.) and AlexaFluor 488 alkyne **19** (1.5 equiv. per N_3) in PBS buffer (10 mM, pH 7.4) was degassed under an argon atmosphere for ~15 min. Cu-power (10 equiv. per N_3) was added under an argon atmosphere and the reaction mixture was vigorously stirred for additional ~3 h at room temperature. The solution was filtered through a two-micron filter and the crude product was purified by C-18 Sep-pak chromatography using H_2O to MeOH/H_2O eluent to afford the desired conjugate as a reddish-colored powder after lyophilization.

Synthesis of conjugate 16

Conjugate **16** was obtained through coupling of compound **15** (0.60 mg, 0.89 μmol, 1.0 equiv.) and lactose amine **6** (1.65 mg, 3.12 μmol, 3.5 equiv.) with NHS-activated PEG **13** (10 mg, 0.89 μmol, 1 equiv.) following the general procedure for conjugation of compound **15** and amine-terminated carbohydrate. Yield: (10.54 mg, 90%). Substitution of compound **15** and amine **6** with the PEG scaffold was determined by ^{1}H NMR integration of the underlined peaks shown below to be GD10/lactose/PEG = 0.95 : 3.05 : 1. ^{1}H NMR (500 MHz, D_2O): δ 7.78–7.58 (m, 2H), 7.38–7.30 (m, 1H), 4.52 (d, J = 8.0 Hz, 1H), 4.50 (d, J = 8.0 Hz, 1H), 4.25 (q, J = 6.0 Hz, 1H), 4.01 (t, J = 6.0 Hz, 2H), 3.98–3.90 (m, 4H), 3.90–3.61 (band, PEG–CH_2–, GD10 CH_2–, sugar–CH, 274H), 3.45–3.43 (band, PEG–CH_2–, 8H), 3.37–3.34 (m, 2H), 3.16–3.09 (m, 2H), 3.07–3.03 (m, 2H), 2.97–2.90 (m, 2H), 2.74 (t, J = 7.8 Hz, 2H), 2.64 (t, J = 6.0 Hz, 2H), 2.70–2.65 (m, 2H), 2.59 (bs, PEG–$COCH_2CH_2CO$–, 4H), 2.34–2.26 (m, 2H), 2.10–2.00 (m, 1H), 1.80–1.73 (m, 2H), 1.68–1.61 (m, 8H), 1.42–1.31 (bs, 14H); ^{13}C NMR (125 MHz, D_2O): δ 182.48, 175.48 (2CO), 174.92, 164.73, 163.87, 147.49, 103.91, 103.02, 79.42, 76.33, 75.73, 75.46, 73.83, 73.52, 72.70, 71.93, 71.65, 71.56 (2C), 70.57 (PEG–CH_2–), 69.82 (2C), 69.52, 69.32, 67.99, 67.80, 67.64, 65.41, 64.33, 61.99 (2C), 61.34, 61.10, 54.91, 51.82, 51.64, 49.84, 46.04, 39.95, 39.71, 38.88, 36.69, 32.19, 32.04, 31.85, 31.35, 29.71, 29.34, 29.16, 29.02, 28.85, 28.59, 25.97, 23.36, 19.77, 12.57; ^{19}F NMR (400 MHz, D_2O): δ −75.51; the MALDI-TOF spectrum showed the average mass centered at 13.0 kDa and expected average mass was 12.9 kDa.

Synthesis of conjugate 17

Conjugate **17** was obtained through coupling of amine **15** (0.81 mg, 1.20 μmol, 1.35 equiv.) and A-type II amine **7** (2.87 mg, 3.12 μmol, 3.5 equiv.) with NHS-activated PEG **13** (10 mg, 0.89 μmol, 1 equiv.) following the general procedure for conjugation of compound **16**. Yield: (11.30 mg, 89%). Substitution of the compound **15** and amine **7** with the PEG scaffold was determined by ^{1}H NMR integration of the underlined peaks shown below to be GD10/A-type II/PEG = 1.03 : 2.97 : 1. ^{1}H NMR (500 MHz, D_2O): δ 7.69–7.62 (m, 1H), 7.61–7.48 (m, 1H), 7.28–7.21 (m, 1H), 4.40 (d, J = 3.6 Hz, 1H), 5.23 (d, J = 3.0 Hz, 1H), 4.65 (d, J = 7.6 Hz, 1H), 4.55 (d, J = 8.0 Hz, 2H), 4.42–4.40 (m, 1H), 4.37 (d, J = 6.6 Hz, 1H), 4.31–4.28 (m, 4H), 4.04 (t, J = 6.0 Hz, 2H), 3.97–3.94 (m, 4H), 3.89–3.67 (band, PEG–CH_2–, GD10 CH_2–, sugar–CH, 271H), 3.64 (bs, 4H), 3.56 (bs, 4H), 3.51–3.48 (m, 2H), 3.45–3.43 (band, PEG–CH_2–, GD10–CH_2, 10H), 3.16–3.09 (m, 2H), 3.07–3.03 (m, 2H), 2.97–2.90 (m, 2H), 2.74 (t, J = 7.8 Hz, 2H), 2.64 (t, J = 7.0 Hz, 2H), 2.70–2.65 (m, 2H), 2.59 (bs, PEG–$COCH_2CH_2CO$–, 4H), 2.30–2.26 (m, 2H), 2.10–2.00 (m, 1H), 2.09 (s, 6H, NHAc), 1.81–1.72 (m, 2H), 1.65–1.60 (m, 6H), 1.43 (bs, 2H), 1.42–1.31 (bs, 14H), 1.30 (d, J = 6.0 Hz, 3H); ^{13}C NMR (125 MHz, D_2O): δ 175.75, 174.62 (2CO), 175.57 (2CO), 175.23, 164.74, 163.73, 147.46, 135.63, 102.08, 101.04, 99.61, 92.30, 79.17, 77.25, 76.65, 76.33, 76.14, 75.72, 73.38 (2C), 72.68, 72.05, 71.55, 71.65 (2C), 70.57 (PEG–CH_2–), 69.82 (2C), 69.46, 68.77, 68.65, 67.82, 65.42, 64.01, 62.28 (2C), 62.14 (2C), 61.19, 56.41 (2C), 51.82, 50.49 (2C), 46.04, 39.95 (PEG–CH_2–), 39.71 (2C), 38.88, 36.69, 32.18, 31.35 (2C), 29.72, 29.30, 28.88, 26.04, 22.93, 19.17, 16.16; ^{19}F NMR (400 MHz, D_2O): δ −75.54; the MALDI-TOF spectrum showed the average mass centered at 14.1 kDa and expected average mass was 14.0 kDa.

Synthesis of conjugate 18

Conjugate **18** was obtained through coupling of compound **15** (0.68 mg, 1.01 μmol, 1.05 equiv.) and 6′-sialyllactose amine **8** (2.76 mg, 3.37 μmol, 3.5 equiv.) with NHS-activated PEG **13** (10.8 mg, 0.96 μmol, 1 equiv.) following the general procedure

for conjugation of compound **16**. Yield: (12.0 mg, 90%). Substitution of the compound **15** and amine **8** with the PEG scaffold **13** was determined by ^{1}H NMR integration of the underlined peaks shown below to be GD10/6′-sialyllactose/PEG = 1.0 : 3.0 : 1. ^{1}H NMR (500 MHz, D_2O): δ 7.66–7.60 (m, 2H), 7.51–7.20 (m, 1H), 4.43 (d, J = 8.4 Hz, 1H), 4.38 (d, J = 8.0 Hz, 1H), 4.01 (t, J = 6.0 Hz, 2H), 3.88–3.82 (m, 2H), 3.84–3.82 (m, 4H), 3.66–3.57 (band, PEG–CH_2–, GD10 CH_2–, sugar–CH, 282H), 3.48–3.45 (m, 4H), 3.34 (t, J = 7.0 Hz, 1H), 3.30 (band, PEG–CH_2–, GD10–CH_2, 8H), 3.18–3.10 (m, 2H), 3.06–3.00 (m, 2H), 2.98–2.91 (m, 2H), 2.64 (t, J = 7.6 Hz, 2H), 2.54 (t, J = 7.0 Hz, 2H), 2.70–2.65 (m, 1H), 2.49 (bs, PEG–$COCH_2CH_2CO$–, 4H), 2.32–2.24 (m, 2H), 1.98 (s, 3H, NHAc), 1.86–1.82 (m, 2H), 1.69 (t, J = 15 Hz, 1H), 1.58–1.50 (m, 6H), 1.29 (bs, 14H); ^{13}C NMR (125 MHz, D_2O): δ 175.88 (2CO), 175.65 (2CO), 175.58 (2CO), 174.40, 164.04, 162.73, 147.43, 135.60, 104.20, 102.89, 101.28, 80.68, 75.70, 74.60, 74.65, 73.72, 73.52, 73.35, 72.73, 71.77, 71.63, 71.55 (2C), 70.56 (PEG–CH_2–), 69.81 (2C), 69.48, 69.30, 64.51, 63.63, 61.29, 52.77, 49.83 (2C), 46.04, 41.06, 39.95 (2C), 39.70, 32.19 (2C), 32.04, 31.34, 29.70 (2C), 29.33, 29.15, 28.85, 25.97, 23.04, 16.17; ^{19}F NMR (400 MHz, D_2O): δ −75.54; the MALDI-TOF spectrum showed the average mass centered at 13.8 kDa and expected average mass was 13.7 kDa.

Synthesis of conjugate 20

Conjugate **20** was obtained through CuAAC coupling of compound **16** (8.0 mg, 0.61 μmol, 1 equiv.) and commercially available AF alkyne **19** (0.67 mg, 0.92 μmol, 1.5 equiv.) following the general procedure for CuAAC ligation. Yield: (7.10 mg, 84%). Substitution of compound **20** was determined by ^{1}H NMR integration of the underlined peaks shown below to be (GD10 + AF)/Lac/PEG = 1 : 3. ^{1}H NMR (500 MHz, D_2O): δ 8.24 (s, 0.15H), 8.19 (s, 0.30H), 8.14–8.00 (m, 0.1H), 8.00 (s, 0.5H, triazole H), 7.71 (m, 0.15 H), 7.58–7.54 (m, 0.5H), 7.48 (d, J = 7.2 Hz, 0.30 H), 7.25 (d, J = 7.2 Hz, 0.30H), 7.15–7.11 (m, 0.30H), 6.96 (d, J = 7.2 Hz, 0.10H), 6.90 (d, J = 7.2 Hz, 0.50H), 4.48 (d, J = 8.0 Hz, 1H), 4.46 (d, J = 8.0 Hz, 1H), 4.28 (q, J = 6.0 Hz, 1H), 3.98 (dd, J = 3.6, 8.0 Hz, 1H), 3.93–3.91 (m, 2H), 3.81–3.79 (m, 4H), 3.76–3.62 (band, PEG–CH_2–, GD10 CH_2–, sugar–CH, 286H), 3.56–3.54 (m, 2H), 3.51(band, PEG–CH_2–, 4H), 3.40–3.39 (m, 4H), 3.31 (t, J = 6.0 Hz, 2H), 3.12–3.09 (m, 1H), 3.01–2.99 (m, 1H), 2.96–2.90 (m, 1H), 2.80 (s, 1H), 2.70 (t, J = 4.6 Hz, 2H), 2.60 (t, J = 6.0 Hz, 2H), 2.60–2.57 (m, 2H), 2.55 (bs, PEG–$COCH_2CH_2CO$–, 4H), 2.08–2.02 (m, 1H), 1.90–1.86 (m, 2H), 1.79–1.74 (m, 2H), 1.64–1.61 (m, 8H), 1.42–1.31 (bs, 14H); ^{13}C NMR (125 MHz, D_2O): δ 175.64 (2CO), 175.62, 174.58 (2C), 103.91, 103.01, 79.41, 76.33, 75.73, 75.45, 73.83, 73.51, 72.69, 71.93, 71.67, 71.55 (2C), 70.56 (PEG–CH_2–), 70.40 (2C), 69.82 (2C), 69.52, 69.32, 67.99, 67.80, 67.64, 65.41, 64.34, 61.99 (2C), 61.34, 61.10, 54.91, 51.65, 51.64, 49.83, 46.04, 39.96 (2C), 39.70, 38.88, 36.69, 34.27, 32.18, 32.16, 32.04, 31.35, 29.70 (2C), 29.32, 29.14, 29.02, 28.83, 28.59, 25.96, 22.80, 19.78; ^{19}F–C NMR (400 MHz, D_2O): δ −75.58; the MALDI-TOF spectrum showed the average mass centered at 13.6 kDa and expected average mass was 13.7 kDa.

Synthesis of conjugate 21

Conjugate **21** was obtained through CuAAC coupling of compound **17** (8.4 mg, 0.60 μmol, 1 equiv.) and commercially available AF alkyne **19** (0.66 mg, 0.91 μmol, 1.5 equiv.) following the general procedure for CuAAC ligation. Yield: (7.10 mg, 80%). Substitution of compound **21** was determined by ^{1}H NMR integration of the underlined peaks shown below to be (GD10 + AF)/AII/PEG = 1 : 3. ^{1}H NMR (500 MHz, D_2O): δ 8.24 (s, 0.15H), 8.12–8.08 (m, 0.1H), 8.00 (s, 0.5H,triazole H), 7.91 (d, J = 7.2 Hz, 0.15 H), 7.68–7.60 (m, 0.5H), 7.60 (d, J = 7.2 Hz, 0.30 H), 7.55–7.50 (m, 1H), 7.29–7.26 (m, 0.3H), 7.04–7.02 (m, 0.15H), 5.40 (d, J = 4.0 Hz, 1H), 5.23 (d, J = 3.6 Hz, 1H), 4.65 (d, J = 7.6 Hz, 1H), 4.55 (d, J = 8.0 Hz, 1H), 4.44–4.40 (m, 1H), 4.37 (d, J = 6.6 Hz, 1H), 4.30 (d, J = 3.6 Hz, 1H), 4.28 (bs, 2H), 4.18 (q, J = 6.0 Hz, 1H), 4.05 (bs, 2H), 4.02 (bs, 2H), 3.97–3.94 (m, 4H), 3.89 (bs, 4H), 3.83–3.66 (band, PEG–CH_2–, GD10 CH_2–, sugar–CH, 269H), 3.64–3.62 (m, 4H), 3.56 (bs, 4H), 3.50–3.48 (m, 2H), 3.45–3.43 (m, 6H), 3.28–3.24 (m, 2H), 3.25–3.21 (m, 1H), 3.14–3.13 (m, 1H), 3.07–3.05 (m, 1H), 2.98–2.2.96 (m, 1H), 2.92–2.90 (m, 1H), 2.85 (s, 1H), 2.74 (t, J = 6.5 Hz, 2H), 2.70–2.65 (m, 2H), 2.64 (t, J = 7.0 Hz, 2H), 2.59 (bs, PEG–$COCH_2CH_2CO$–, 4H), 2.33–2.26 (m, 2H), 2.09 (s, 6H, NHAc), 1.82–1.80 (m, 1H), 1.69–1.60 (m, 6H), 1.38–1.36 (m, 14H), 1.32 (bs, 18H); ^{13}C NMR (125 MHz, D_2O): δ 175.76, 174.64 (2CO), 175.58 (2CO), 175.25, 164.74, 163.73, 102.08, 101.04, 99.61, 92.30, 79.17, 77.24, 76.65, 76.33, 76.13, 75.72, 73.38 (2C), 72.69 (2C), 72.05, 71.55 (2C), 71.65 (2C), 70.56 (PEG–CH_2–), 69.81 (2C), 69.46, 69.32, 68.76, 68.65, 67.82, 65.42, 64.01, 62.28 (2C), 62.15 (2C), 61.34, 61.19, 56.41 (2C), 51.82, 51.81, 51.80, 50.48 (2C), 46.04, 39.95 (PEG–CH_2–), 39.70 (2C), 38.89, 36.69, 32.18 (2C), 32.04, 31.35, 30.76, 29.71, 29.53, 29.29, 29.25, 29.02, 28.87, 26.03, 22.26, 16.16; ^{19}F–C NMR (400 MHz, D_2O): δ −75.50; the MALDI-TOF spectrum showed the average mass centered at 14.2 kDa and expected average mass was 14.7 kDa.

Synthesis of conjugate 22

Conjugate **22** was obtained through CuAAC coupling of compound **18** (7.0 mg, 0.50 μmol, 1 equiv.) and commercially available AF alkyne **19** (0.55 mg, 0.76 μmol, 1.5 equiv.) following the general procedure for CuAAC ligation. Yield: (6.12 mg, 83%). Substitution of compound **22** was determined by ^{1}H NMR integration of the underlined peaks shown below to be (GD10 + AF)/6′SL/PEG = 1 : 3. ^{1}H NMR (500 MHz, D_2O): δ 7.66–7.60 (m, 2H), 7.51–7.20 (m, 1H), 4.53 (d, J = 8.0 Hz, 1H), 4.48 (d, J = 8.0 Hz, 1H), 4.42 (q, J = 6.0 Hz, 1H), 3.90–3.88 (m, 2H), 3.86–3.82 (m, 4H), 3.80–3.65 (band, PEG–CH_2–, GD10 CH_2–, sugar–CH, 279H), 3.64–3.60 (m, 4H), 3.59 (bs, 4H), 3.34 (t, J = 7.0 Hz, 2H), 3.18–3.10 (m, 2H), 3.44 (t, J = 7.6 Hz, 2H), 3.28–3.24 (m, 2H), 3.25–3.21 (m, 1H), 3.14–3.13 (m, 1H), 3.07–3.05 (m, 1H), 2.98–2.2.97 (m, 1H), 2.92–2.90 (m, 1H), 2.85 (s, 1H), 2.80–2.75 (m, 1H), 2.74 (t, J = 7.6 Hz, 2H), 2.64 (t, J = 7.6 Hz, 2H), 2.65–2.62 (m, 1H), 2.59 (bs, PEG–$COCH_2CH_2CO$–, 4H), 2.32–2.24 (m, 2H), 2.08 (s, 3H, NHAc), 1.80 (t, J = 15 Hz, 1H), 1.68–1.60 (m, 6H), 1.39–1.33 (m, 12H), 1.32 (bs, 14H); ^{13}C NMR (125 MHz, D_2O): δ 179.89, 176.23, 175.66, 174.59 (2CO), 171.43,

175.25, 164.74, 163.74, 123.35, 122.75, 116.78, 109.97, 104.20, 102.89, 80.67, 79.17, 75.70, 75.611, 73.72, 73.51, 73.35, 72.76, 72.74, 71.77, 71.76, 71.55 (2C), 70.56 (PEG–CH_2–), 69.81 (2C), 69.48, 69.32, 64.52, 64.50, 63.62, 62.34 (2C), 52.77 (2C), 48.21, 47.65, 46.04, 41.10, 39.95 (PEG–CH_2–), 39.70, 32.19 (2C), 32.04, 31.35, 30.78, 29.70 (2C), 29.33, 29.15, 29.85, 25.97, 23.03, 14.91, 9.19; ^{19}F–C NMR (400 MHz, D_2O): δ −75.57; the MALDI-TOF spectrum showed the average mass centered at 14.2 kDa and expected average mass was 14.5 kDa.

MALDI-TOF mass spectrometry analysis

Samples were dissolved in water and an aliquot of 1 μL of sample was spotted onto a Bruker Daltonics MTP ground steel target and air-dried. A 1 μL aliquot of matrix solution was spotted on top of the sample spot and air-dried. The matrix solution consisted of a saturated solution of CHCA (α-cyano-4-hydroxycinnamic acid) or DHB (dihydroxybenzoic acid) in 50% water acetonitrile with 0.1% TFA. Mass spectra were obtained in the positive or negative linear mode of ionization using a Bruker Daltonics (Bremen, Germany) ultrafleXtreme MALDI TOF/TOF mass spectrometer. Data analysis software packages provided by the manufacturer were used for analysis.

Fluorescence polarization (FP) binding assay

The affinity of AG10 analog **23** and the labelled GD10 compound **24** to human TTR in PBS at pH 7.4 in assay buffer was evaluated by direct binding or displacement of an FP probe from the protein using an assay similar to that reported by Penchala *et al.*[21] The affinity of GD10 conjugate **24** to TTR was determined by addition of **24** (2 μL, 1 nM) to serial dilutions of TTR (23 μL, 9.01 μM to 0.017 μM) in freshly prepared assay buffer (PBS pH 7.4, 0.01% Triton, 1% DMSO) in a black 384-well plate at room temperature. Samples were allowed to equilibrate by agitation for 25 min in the dark by covering an aluminum foil. Fluorescence polarization (λ_{ex} 485 nm, λ_{em} 525 nm) was measured using a Cytation 5 cell imaging multi-mode micro plate reader. To evaluate the ability of AG10 analog **23** to act as a competitor to GD10, a complex between hTTR and GD10 conjugate **24** was formed by incubation of a mixture of hTTR (4.0 μM, 18 μL) and GD10 conjugate **24** (1 nM, 2 μL) in a black 384-well plate for 10 min. Serial dilutions of AG10 analog **23** (50 μM to 0.04 μM) were added in aliquots (5 μL) to the hTTR-GD10 complex (25 μL final volume) and allowed to incubate for 25 min at room temperature in the dark. The assay solutions were then briefly centrifuged to disperse air bubbles and then measured for fluorescence polarization. For serum binding experiments, mouse serum was assumed to contain 230 nM murine TTR for the purposes of calculating k_{app}.[31]

Synthesis of fluorescently labelled protein 25

To make the fluorescently labelled alpha-1-acidic glycoprotein (AGP), 2 mg mL^{-1} of the protein solution was prepared in 0.1 M $NaCO_3$ (pH 8.5–9). *N*-Hydroxylsuccinimide-AF dye (Molecular Probes) dissolved in DMSO was then added to the protein solution to a final concentration of 0.05 μg mL^{-1} and the reaction left to proceed at room temperature for 1 h in dark. To quench the reaction, ethanolamine was added to the final concentration of 0.1 M (pH 9–10) for 2 h at 4 °C. To remove the excess unreacted dye, ultracentrifugation with molecular cut-off of 10 kDa was used. The protein solution was diluted to 200 μL using PBS, the solution was spun at 14 000×*g* at 4 °C for 10 min; this process was repeated three times. The final concentration of the proteins and level of labeling was determined by UV absorbance to be 1 mg mL^{-1} protein with ∼1.2 dye : protein ratio.

Murine *in vivo* clearance model

Wild-type BALB/c mice (8–18 weeks of age, 4 male and 3 female) were injected i.v. *via* the saphenous vein with either conjugate **9**, **10**, **11**, **20**, **21**, **22**, or **25** at 300 μg/100 μL PBS buffer (pH 7.4). The concentration used for the glycoconjugates was based on previous ABO tolerance studies in BALB wild-type mice using A-antigen expressing erythrocytes.[29] For replicate measurements mice were injected either with conjugates **10** or **21**. Blood samples were collected from tail bleeds pre-injection and at 10 min, 1, 2, 4, 24, 48 and 96 h post-injection.

Blood samples were centrifuged at 4000×*g* for 5–10 min and 10 μL aliquots of serum diluted with 220 μL of buffer (PBS pH 7.4) at room temperature. Fluorescence (emission scan: λ_{ex} = 494 nm and λ_{em} = 502–700 nm and excitation scan: λ_{ex} = 400–500 nm and λ_{em} = 518 nm) was measured using a spectrophotometer reader (PTI QM-400 and PTI Horiba Scientific systems) for respective conjugates (**9–11**, **20**, **21**, and **25**) and (**11** and **22**). For non-injected mouse serum samples, a fluorescence signal was not observed and these were considered as 'blank' samples. All half-life measurements were performed on two separate animals, with triplicate samples at each time point. Fluorescence changes were determined by height of the emission signal at 519–520 nm. Half-life of the AF labeled (λ_{ex} = 496 nm and λ_{em} = 519 nm) conjugates was determined from plotting the post-injection time points and intensity of the emission signal. Half-life was derived through plotting the data on GraphPad prism and fitting the results to a non-linear regression and exponential one-phase decay.

Whole body/organ imaging of GC in mice

C3H/He mice were injected within 24 h of birth in the superficial temporal vein (30-gauge needle) with compound **21** dissolved in PBS at the indicated doses. At days one and six post-injection, mice were anesthetized on ice for whole body imaging. Injected mice were imaged next to non-injected littermate controls to distinguish compound **21** signal from autofluorescence. Mice were imaged with an Olympus OV100 small animal imaging system using a Hamamatsu ImagEM camera with automatic exposure. The objective lens for image acquisition was 0.14X/0.039 and the excitation and emission filters were Ex BP460-490/Em BA510-550. Images were acquired using the native OV100 software. As overlying tissue blocked fluorescent signals, freshly dissected organs were imaged in the unfixed state next to those from non-injected littermate controls.

Synthesis of conjugate 27

Conjugate **27** was obtained through CuAAC coupling of compounds **17** (10.0 mg, 0.71 μmol, 1 equiv.) and 6′-sialyllactoside

26[14] (0.71 mg, 1.07 μmol, 1.5 equiv.) following the general procedure for CuAAC ligation. Yield: (8.95 mg, 80%). ^{1}H NMR (500 MHz, D_2O): δ 8.00 (s, 1H, triazole H), 7.67 (d, J = 7.6 Hz, 1H), 7.59 (bs, 1H), 7.59 (m, 1H), 5.40 (d, J = 4.0 Hz, 1H), 5.23 (d, J = 3.6 Hz, 1H), 4.65 (d, J = 7.6 Hz, 1H), 4.55 (d, J = 8.0 Hz, 1H), 4.44–4.40 (m, 1H), 4.43 (d, J = 12.6 Hz, 1H, H-1'), 4.38 (d, J = 12.0 Hz, 1H, H-1), 4.37 (d, J = 6.6 Hz, 1H), 4.30 (d, J = 3.6 Hz, 1H), 4.28 (bs, 2H), 4.18 (q, J = 6.0 Hz, 1H), 4.05 (bs, 2H), 4.02 (bs, 2H), 3.97–3.94 (m, 4H), 3.89 (bs, 4H), 3.83–3.66 (band, PEG–CH_2–, GD10 CH_2–, sugar–CH, 264H), 3.64–3.62 (m, 4H), 3.56 (bs, 4H), 3.50–3.48 (m, 2H), 3.45–3.43 (m, 6H), 3.28–3.24 (m, 2H), 3.25–3.21 (m, 1H), 3.17–3.11 (m, 1H), 3.07–3.03 (m, 1H), 2.98–2.2.94 (m, 1H), 2.92–2.90 (m, 1H), 2.85 (s, 1H), 2.74 (t, J = 6.5 Hz, 2H), 2.70–2.65 (m, 2H), 2.66 (dd, J = 6.6, 18.6 Hz, 1H, Heq-3), 2.64 (t, J = 7.0 Hz, 2H), 2.59 (bs, PEG–$COCH_2CH_2CO$–, 4H), 2.33–2.26 (m, 2H), 2.09 (s, 6H, NHAc), 1.98 (s, 3H, NHAc), 1.82–1.80 (m, 1H), 1.69–1.67 (m, 6H), 1.68 (t, J = 18.6 Hz, 1H, Hax-3), 1.38–1.36 (m, 14H), 1.32 (bs, 18H); ^{13}C NMR (125 MHz, D_2O): δ 175.76, 175.64 (2CO), 175.58 (2CO), 175.26 (2CO), 174.34, 161.19, 163.73, 145.69, 134.26, 104.23, 102.08 (2CO), 101.04 (2CO), 99.61, 92.30, 84.92, 80.55, 79.24, 77.24, 76.65, 76.33, 76.14, 75.66, 75.55, 74.48, 75.80, 75.77, 73.87, 73.61, 73.58, 73.38 (2C), 72.69 (2C), 72.05, 71.88, 71.65 (2C), 71.55 (2C), 71.49, 70.92 (2C), 70.56 (PEG–CH_2–), 69.81 (2C), 69.47, 69.36, 69.23, 68.76, 68.65, 67.82, 64.42, 64.01, 62.27, 62.14, 62.0, 61.34, 61.19, 61.00, 56.41 (2C), 52.63, 51.89, 51.63, 51.01, 50.48 (2C), 46.04, 40.94, 39.95 (PEG–CH_2–), 39.70 (2C), 38.89, 36.69, 32.18 (2C), 32.03, 31.34, 29.71, 29.53, 29.25, 29.02, 29.02, 28.87, 26.03, 23.26, 22.93, 22.26, 16.15; ^{19}F–C NMR (400 MHz, D_2O): δ −75.49; the MALDI-TOF spectrum showed the average mass centered at 14.6 kDa and expected average mass was 15.2 kDa.

Fluorescence microscopy and clustering analysis on B cells

A-BCL cells were prepared and grown as previously described.[32] Cells were grown in R10 media supplemented with glutamax and 1% beta-mercaptoethanol added weekly in 12-well plates (Corning, Inc.). Plates were kept in a humidified incubator at 37 °C and 5% CO_2. For single-color fluorescence microscopy experiments, 2×10^6 cells were washed and treated with buffer, conjugate **27** (25 ng mL^{-1}), conjugate **27** and TTR (50 ng mL^{-1}), or conjugate **28** (25 ng mL^{-1})[14] on ice for 1 h, then fixed using 1% PFA on ice for 20 min. Samples were treated with 1 μL mL^{-1} mouse *anti*-human CD22 (clone HIB22, BD Pharmingen) at 4 °C overnight, washed, and stained with goat *anti*-mouse IgG (polyclonal, Sigma-Aldrich) conjugated with AF647 at room temperature for 1 hour. The loading of the fluorophores was approximately 2 dye per protein as determined by spectrophotometry. After washing, samples were transferred to 24-well plates (Corning, Inc.) with 12 mm circular cover glass slides pre-treated with 0.001% poly-L-lysine and spun at 300 × g for 15 min. Cover glass slides with samples were washed, mounted onto microscopy slides with Slowfade Antifade (ThermoFisher), and sealed with Cytoseal 60. Samples were imaged on a laser scanning confocal microscope (Olympus IX81) at 60X. Twenty cells from each condition were chosen for analysis based on transmitted and fluorescence images, in which each image was subjected to similar thresholding levels, and each cluster was analyzed using the particle analysis function on ImageJ.[33] The area of a single pixel in these images was 0.053 μm^2. The areas of each cluster from the analyses were plotted using beanplot in the R statistical package.[30] Analysis of the means and Student's t-test were performed in Graphpad Prism.

Conflicts of interest

There are no conflicts to declare.

Acknowledgements

The authors would like to thank Prof. Todd L. Lowary and Dr Peter Meloncelli for providing advanced synthetic intermediates for the synthesis of human ABO blood group antigens. This work was supported by grants from the Alberta Glycomics Centre (CWC, LJW) and the Natural Sciences and Engineering Research Council of Canada (NSERC; CWC RGPIN-2020-04371).

References

1 Y. M. Chabre and R. Roy, Multivalent glycoconjugate syntheses and applications using aromatic scaffolds, *Chem. Soc. Rev.*, 2013, **42**, 4657–4708.
2 P. H. Seeberger and D. B. Werz, Synthesis and medical applications of oligosaccharides, *Nature*, 2007, **446**, 1046–1051.
3 N. Jayaraman, Multivalent ligand presentation as a central concept to study intricate carbohydrate-protein interactions, *Chem. Soc. Rev.*, 2009, **38**, 3463–3483.
4 Y. M. Chabre and R. Roy, Design and creativity in synthesis of multivalent neoglycoconjugates, *Adv. Carbohydr. Chem. Biochem.*, 2010, **63**, 165–393.
5 L. L. Kiessling, J. E. Gestwicki and L. E. Strong, Synthetic Multivalent Ligands as Probes of Signal Transduction, *Angew. Chem., Int. Ed.*, 2006, **45**, 2348–2368.
6 O. Renaudet and R. Roy, Multivalent scaffolds in glycoscience: an overview, *Chem. Soc. Rev.*, 2013, **42**, 4515–4517.
7 P. Costantino, R. Rappuoli and F. Berti, The design of semi-synthetic and synthetic glycoconjugate vaccines, *Expert Opin. Drug Discovery*, 2011, **6**, 1045–1066.
8 R. Braeckman, Pharmacokinetics/ADME of large molecules, *Preclinical Drug Development*, CRC Press, 2nd edn, 2016, pp. 127–151.
9 B. Haraldsson, J. Nyström and W. M. Deen, Properties of the Glomerular Barrier and Mechanisms of Proteinuria, *Physiol. Rev.*, 2008, **88**, 451–487.
10 F. Yamashita and M. Hashida, Pharmacokinetic considerations for targeted drug delivery, *Adv. Drug Delivery Rev.*, 2013, **65**, 139–147.
11 R. Braeckman and B. Meibohm, Pharmacokinetics and pharmacodynamics of peptide and protein drugs, *Pharmaceutical biotechnology*, CRC Press, 2016, pp. 107–135.
12 E. I. Park, Y. Mi, C. Unverzagt, H.-J. Gabius and J. U. Baenziger, The asialoglycoprotein receptor clears

glycoconjugates terminating with sialic acidα2, 6GalNAc, *Proc. Natl. Acad. Sci. U. S. A.*, 2005, **102**, 17125–17129.

13 C. I. C. Crucho, P. Correia-da-Silva, K. T. Petrova and M. T. Barros, Recent progress in the field of glycoconjugates, *Carbohydr. Res.*, 2015, **402**, 124–132.

14 G. C. Daskhan, H.-T. T. Tran, P. J. Meloncelli, T. L. Lowary, L. J. West and C. W. Cairo, Construction of Multivalent Homo- and Heterofunctional ABO Blood Group Glycoconjugates Using a Trifunctional Linker Strategy, *Bioconjugate Chem.*, 2018, **29**, 343–362.

15 A. H. Courtney, E. B. Puffer, J. K. Pontrello, Z. Q. Yang and L. L. Kiessling, Sialylated multivalent antigens engage CD22 in trans and inhibit B cell activation, *Proc. Natl. Acad. Sci. U. S. A.*, 2009, **106**, 2500–2505.

16 M. K. O'Reilly, B. E. Collins, S. Han, L. Liao, C. Rillahan, P. I. Kitov, D. R. Bundle and J. C. Paulson, Bifunctional CD22 Ligands use multimeric immunoglobulins as protein scaffolds in assembly of immune complexes on B cells, *J. Am. Chem. Soc.*, 2008, **130**, 7736–7745.

17 D. S. Jones, M. J. Branks, M. A. Campbell, K. A. Cockerill, J. R. Hammaker, C. A. Kessler, E. M. Smith, A. Tao, H. T. Ton-Nu and T. Xu, Multivalent Poly(ethylene glycol)-Containing Conjugates for in Vivo Antibody Suppression, *Bioconjugate Chem.*, 2003, **14**, 1067–1076.

18 H. Borel and Y. Borel, A novel technique to link either proteins or peptides to gammaglobulin to construct tolerogens, *J. Immunol. Methods*, 1990, **126**, 159–168.

19 M. D. Mannie and I. I. A. D. Curtis, Tolerogenic vaccines for Multiple Sclerosis, *Hum. Vaccines Immunother.*, 2013, **9**, 1032–1038.

20 K. A. Cockerill, G. M. Iverson, D. S. Jones and M. D. Linnik, Therapeutic Potential of Toleragens in the Management of Antiphospholipid Syndrome, *BioDrugs*, 2004, **18**, 297–305.

21 S. C. Penchala, M. R. Miller, A. Pal, J. Dong, N. R. Madadi, J. Xie, H. Joo, J. Tsai, P. Batoon, V. Samoshin, A. Franz, T. Cox, J. Miles, W. K. Chan, M. S. Park and M. M. Alhamadsheh, A biomimetic approach for enhancing the in vivo half-life of peptides, *Nat. Chem. Biol.*, 2015, **11**, 793–798.

22 S. C. Penchala, S. Connelly, Y. Wang, M. S. Park, L. Zhao, A. Baranczak, I. Rappley, H. Vogel, M. Liedtke, R. M. Witteles, E. T. Powers, N. Reixach, W. K. Chan, I. A. Wilson, J. W. Kelly, I. A. Graef and M. M. Alhamadsheh, AG10 inhibits amyloidogenesis and cellular toxicity of the familial amyloid cardiomyopathy-associated V122I transthyretin, *Proc. Natl. Acad. Sci. U. S. A.*, 2013, **110**, 9992–9997.

23 M. M. Alhamadsheh, S. Connelly, A. Cho, N. Reixach, E. T. Powers, D. W. Pan, I. A. Wilson, J. W. Kelly and I. A. Graef, Potent Kinetic Stabilizers That Prevent Transthyretin-Mediated Cardiomyocyte Proteotoxicity, *Science Translational Medicine 3*, 2011, 97ra81.

24 M. Miller, A. Pal, W. Albusairi, H. Joo, B. Pappas, M. T. Haque Tuhin, D. Liang, R. Jampala, F. Liu, J. Khan, M. Faaij, M. Park, W. Chan, I. Graef, R. Zamboni, N. Kumar, J. Fox, U. Sinha and M. Alhamadsheh, Enthalpy-Driven Stabilization of Transthyretin by AG10 Mimics a Naturally Occurring Genetic Variant That Protects from Transthyretin Amyloidosis, *J. Med. Chem.*, 2018, **61**, 7862–7876.

25 A. Pal, W. Albusairi, F. Liu, M. T. H. Tuhin, M. Miller, D. Liang, H. Joo, T. U. Amin, E. A. Wilson, J. S. Faridi, M. Park and M. M. Alhamadsheh, Hydrophilic Small Molecules That Harness Transthyretin To Enhance the Safety and Efficacy of Targeted Chemotherapeutic Agents, *Mol. Pharm.*, 2019, **16**, 3237–3252.

26 A. Dondoni, The Emergence of Thiol–Ene Coupling as a Click Process for Materials and Bioorganic Chemistry, *Angew. Chem., Int. Ed.*, 2008, **47**, 8995–8997.

27 Q. Wan, J. Chen, G. Chen and S. J. Danishefsky, A Potentially Valuable Advance in the Synthesis of Carbohydrate-Based Anticancer Vaccines through Extended Cycloaddition Chemistry. *The*, *J. Org. Chem.*, 2006, **71**, 8244–8249.

28 R. Bascom, K. Tao, S. Tollenaar and L. West, Imaging Tolerance Induction in the Classic Medawar Neonatal Mouse Model: Active Roles of Multiple F1-Donor Cell Types, *Am. J. Transplant.*, 2015, **15**, 2346–2363.

29 B. Motyka, J. Fersovich, B. Lamarche, M. Sosniuk, I. Adam, J. Pearcey, K. Tao, C. W. Cairo, P. J. Cowan and L. J. West, MHC-Matched A-Expressing Blood Cells Induce ABO Tolerance in Infant and Adult Mice, *Transplantation*, 2018, **102**, S292.

30 P. Kampstra, Beanplot: A boxplot alternative for visual comparison of distributions, *J. Stat. Softw.*, 2008, **28**, 1–9.

31 I. Gonçalves, C. H. Alves, T. Quintela, G. Baltazar, S. Socorro, M. J. Saraiva, R. Abreu and C. R. A. Santos, Transthyretin is up-regulated by sex hormones in mice liver, *Mol. Cell. Biochem.*, 2008, **317**, 137–142.

32 A. M. Slaney, I. E. Dijke, M. Jeyakanthan, C. Li, L. Zou, P. Plaza-Alexander, P. J. Meloncelli, J. A. Bau, L. L. Allan, T. L. Lowary, L. J. West, C. W. Cairo and J. M. Buriak, Conjugation of A and B Blood Group Structures to Silica Microparticles for the Detection of Antigen-Specific B Cells, *Bioconjug. Chem.*, 2016, **27**, 705–715.

33 C. A. Schneider, W. S. Rasband and K. W. Eliceiri, NIH Image to ImageJ: 25 years of image analysis, *Nat. Methods*, 2012, **9**, 671–675.